ARTICLE NO. 78-1218R

J80-017

20006
20008
30012

Pulsed Laser-Induced Shattering of Water Drops

P. I. Singh* and C. J. Knight*
Avco Everett Research Laboratory, Everett, Mass.

Water droplets with radii ranging from 0.1 to 1.5 mm were irradiated by 10 μs pulses from a pulsed CO_2 laser ($\lambda = 10.6$ μm) operating at intensities between 10^4 and 6×10^5 W/cm^2. The absorption length (~ 10 μm) was much smaller than the droplet radii so that the laser-drop interaction was a surface phenomenon leading to overpressures on the irradiated front surface which exceeded surface tension forces by at least an order of magnitude. However, these high overpressures did not cause all droplets to shatter. There appeared to be a critical laser fluence of 0.8-2.5 J/cm^2 required for shattering, essentially independent of radius. Above the critical fluence the drops were deformed into thin liquid films with subsequent breakup into smaller satellite droplets. For fixed pulse duration the shattering time decreases with increasing intensity and with decreasing initial drop size. Simple scaling and energy conservation relations are used to predict the radii of the satellite droplets and to estimate a critical impulse parameter.

Introduction

THE propagation of high energy laser radiation under adverse weather conditions is of concern in the utilization of such laser devices. An earlier paper[1] reported on the phenomenology of nonlinear laser interactions, at CO_2 laser wavelengths, with water aerosols. In the present paper we discuss the results of a primarily experimental program on the irradiation of large water drops (i.e., rain) by a pulsed CO_2 laser operating at 10.6 μm. Of concern are cases where the total absorbed laser flux is much less than the energy required to vaporize the drop, but which may be sufficient to deform and shatter the drops into smaller satellite droplets. The shattering of drops is of significance in propagation scenarios since it effectively alters the aerosol size distribution along the beam path, and hence the extinction coefficient. Although experiments have been performed only with a CO_2 laser, the shattering phenomenon is also expected to occur at other infrared wavelengths.

The experiments to be discussed here involve droplet radii which are large compared to the absorption length in water, which is about 10^{-3} cm at the 10.6 μm wavelength employed. Droplet radii ranged from 0.01 to 0.15 cm; the upper bound corresponds roughly to the maximum radius of naturally occurring rain. In addition, the laser fluence used (0.1-6.5 J/cm^2) was small compared to that required to completely vaporize droplets in the size range considered. The latter number is estimated as $4/3\pi R^3\rho h_v/\pi R^2 \sim 33$-$500$ J/cm^2 for a drop radius $R = 0.01$-0.15 cm, where $\rho = 1$ g/cm^3 and $h_v = 2.5$ kJ/g for water. Under these conditions the laser-drop interaction is essentially a surface phenomenon occurring at the irradiated front face, and only a small fraction of the water in the drop is vaporized.

At sufficiently high laser intensities, rapid vaporization will occur on the irradiated front face, which leads to an effective overpressure $p_e = p_{surface} - P_{ambient}$ at that surface due to momentum recoil effects. Certain aspects of that process are discussed in Ref. 2. If the situation involved steady-state pressure loading, the drop would be expected to deform and shatter in a manner analogous to Weber number scaling arguments,[3] when p_e sufficiently exceeds the surface tension forces:

$$p_e > 2\sigma/R \tag{1}$$

where σ is the coefficient of surface tension (~ 75 dyne/cm for water). As an example, a drop with $R = 0.01$ cm would be expected to shatter under a steady loading exceeding 30 Torr. This critical pressure should vary inversely with R in accordance with Eq. (1). In the pulsed laser experiments, large droplets were observed not to shatter with an overpressure estimated to exceed 1 atm for short time intervals. The physical explanation of the droplet shattering threshold in these experiments is clearly not contained in Eq. (1).

An alternative explanation involves a critical impulse for shattering, and this is found to be more in accord with the experimental results. An impulse criterion has apparently not been established previously. Dimensional arguments are used to establish the relevant nondimensional group characterizing instantaneous impulsive loading on one face of a droplet. The experiments described below were then used to roughly establish the critical value for that nondimensional group. An energy conservation relation is also developed and used to predict the size of the satellite droplets after shattering. Comparison with experiments show qualitative agreement. The energy conservation relations can be used to establish a lower bound on the critical impulse parameter which is a factor of 3-6 lower than the experimentally estimated value.

Experimental Setup

The experiments were conducted using a collimated beam from a pulsed electric discharge CO_2 laser with the setup shown in Fig. 1. Average laser intensities were varied, using attenuation screens, between 9×10^3 and 6.5×10^5 W/cm^2 at the plane of the droplets. The spatial distribution corresponded to the near field of a top-hat input profile. Without attenuation screens, this was determined by array measurements in related work reported in Ref. 4. Spatial uniformity behind the screens was indicated by burn patterns on thermosensitive paper. Over the scale size of the droplets, however, we have little quantitative information on spatial uniformity, and it is conceivable that there is a variation factor of two in local intensity due to diffraction effects. The droplets are in the near field of the attenuation screens due to space limitations for the experiments. The beam area was much larger than the cross-sectional area of the largest droplets tested.

Presented as Paper 78-1218 at the AIAA 11th Fluid and Plasma Dynamics Conference, Seattle, Wash., July 10-12, 1978; submitted Aug. 4, 1978; revision received July 17, 1979.

Index categories: Lasers; Hydrodynamics; Multiphase Flows.

*Principal Research Scientist. Member AIAA.

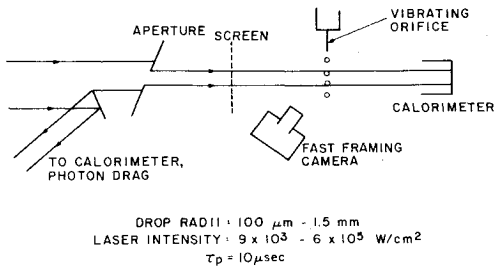

Fig. 1 Experimental setup.

The temporal pulse shape is shown in Fig. 2. There was a gain-switch spike of 0.3-μs duration and an intensity approximately seven times higher than the average. The laser waveform and energy were monitored using photon drag detectors and calorimeters. The pulse length, as determined by the photon drag detectors, was 10 μs. The average intensity I follows from the total energy measured by the calorimeters, the beam area, and the 10-μs pulse duration. That is, I corresponds to an equivalent top-hat temporal pulse shape. The spatial profile is also a top-hat distribution, as already discussed. In the intensity range considered, calorimeters can be expected to measure the beam energy within $\pm 5\%$.

The history of the irradiated drops was monitored by a Hycam fast framing camera operating at 10^4 frames/s and a 40-μs frame exposure time. The framing rate was too slow to record events on a time scale comparable to the 10 μs laser pulse, but later droplet response was easily recorded for the larger drops. Due to the framing rate, there is a 100-μs uncertainty as to when the laser pulse actually occurs in a film sequence.

The water drops were generated using a vibrating orifice which allowed drop radii to be varied. The experiments were conducted using distilled, deionized water.

Experimental Results

Experimental results of importance for laser propagation through rain are: a) criterion for drop shattering; 2) time required for drop shattering; 3) final droplet size distribution. These will be discussed in this section.

A threshold for drop shattering was observed. The results are summarized in Fig. 3 vs the average intensity corresponding to an equivalent top-hat beam. Care should be used in interpreting these results because the local laser intensity at a droplet could be different from the beam-averaged value. For this reason the shattering threshold intensity can only be approximately established as 1×10^5 W/cm^2. The associated laser fluence of 1 J/cm^2 is obtained by multiplying by the 10-μs pulse duration. These values appear to be essentially independent of droplet radius on the basis of available data. Above the threshold the drops were deformed into thin liquid films which subsequently broke up into smaller droplets. A typical Hycam camera sequence in Fig. 4 shows the breakup of a 0.13-cm-radius droplet for $I=2.5\times10^5$ W/cm^2.

To better understand the physical processes involved, it is useful to relate the laser intensity to the overpressure on the droplet. An estimate of p_e for a surface normal to the beam can be made if the vapor blowoff is assumed to be sonic:

$$\frac{p_e}{I} \sim \frac{\gamma+1}{\gamma}\frac{\dot{m}c}{\dot{m}h_v} \sim 24\frac{\text{dyne/cm}^2}{\text{W/cm}^2} \qquad (2)$$

where γ is the ratio of specific heats, $\dot{m}$ is the mass flux of vaporized water, c is the sound speed, and h_v is the latent heat of vaporization. The energy required to bring the water at the drop surface to the boiling point can be included in an effective h_v. Detailed calculations using the technique outlined in Ref. 2 show that Eq. (2) is roughly correct for laser intensities $I \geq 10^5$ W/cm^2. The error is 10-15% for $I=10^5$-10^6 W/cm^2, but can be substantially larger below 10^5 W/cm^2 because the vapor blowoff is not sonic.

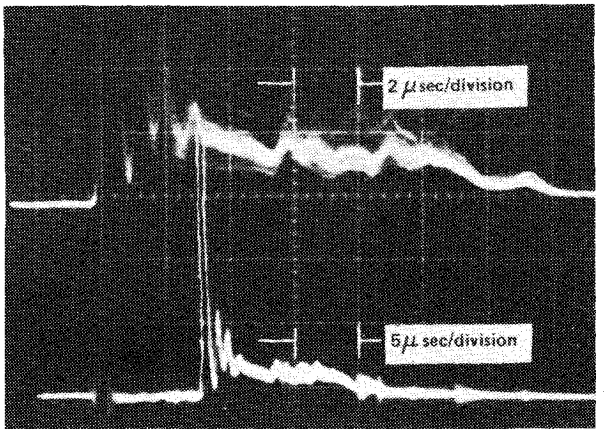

Fig. 2 Laser pulse waveform.

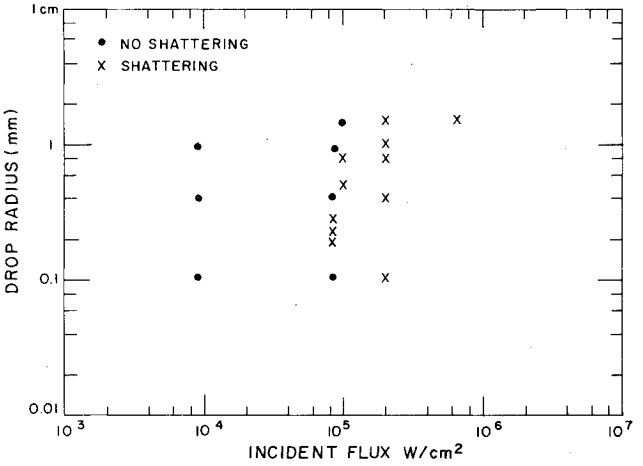

Fig. 3 Drop shattering thresholds ($\tau_p = 10$ μs).

The linear relationship between laser intensity and overpressure in Eq. (2) was used to replot the results of Fig. 3 as overpressure vs drop radius in Fig. 5. Note that p_e should be understood to be the maximum overpressure on the droplet because Eq. (2) applies to a surface normal to the beam. Distribution of overpressure around a spherical droplet will be discussed later. The line $p_e = 2\sigma/R$ is shown. It is clear that the shattering criterion does not involve an overpressure threshold of the sort given in Eq. (1). The other curves in Fig. 5 are based on an impulse threshold criterion and will be discussed later.

We define the shattering time as the time required to go from the initial state to the final droplet formation. It should be understood that identification of the final state is somewhat subjective. Also, there is a 0.1-ms uncertainty as to when the laser pulse occurs, due to the framing rate, that can introduce significant errors in estimated shattering times for smaller drops. With these caveats and within the range of intensities considered, the shattering time depends upon both the laser intensity and the initial drop size. Typical results are shown in Fig. 6 for $I=8\times10^4$ W/cm^2 and $I=2.5\times10^5$ W/cm^2. The shattering time is an important parameter for multiple-pulse propagation because it determines the degree to which the droplet size distribution along the beam path is altered between successive pulses. At typical intensities and pulse repetition rates, rain drops should be completely shattered between pulses.

The final droplet size distribution is a function of both the laser intensity and the initial drop size. The final droplet radii

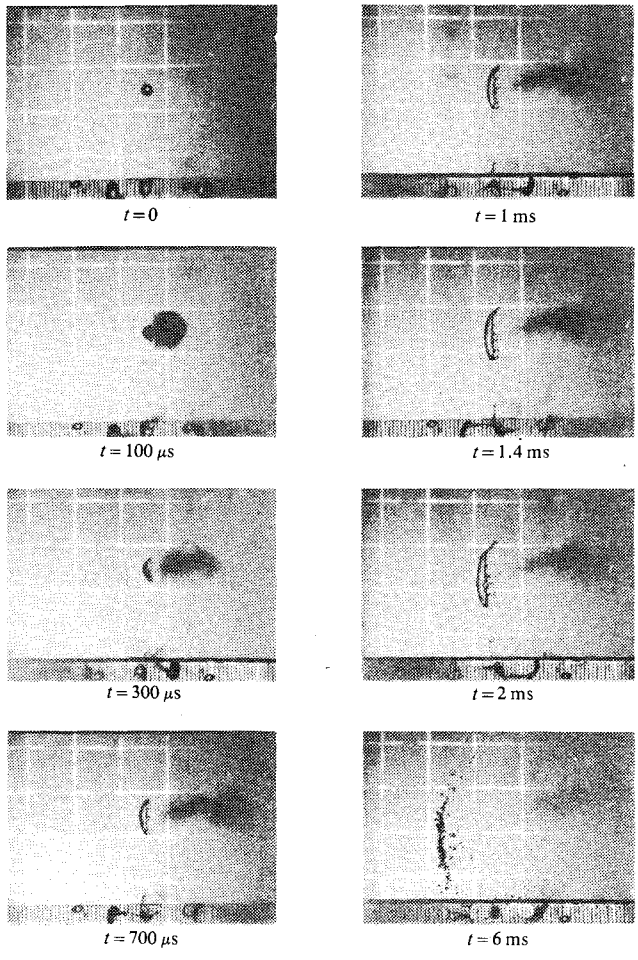

Fig. 4 Fast framing photographs of droplet shattering (scale at bottom is in millimeters).

produced by liquid sheet instabilities decrease with increasing laser intensity and decreasing initial diameter. A histogram of final droplet size distribution for the example shown in Fig. 4 has been constructed and is shown in Fig. 7. A representative sample consisting of about 30% of the final droplet population was used. The initial droplet radius was $R = 0.13$ cm and the incident laser intensity was $I = 2.5 \times 10^5$ W/cm^2. From the size distributions, histograms for surface energy and volume distributions have been computed and are also shown in Fig. 7. Although there is a significant range of final droplet radii, the centroids of the various histograms are sufficiently near each other so that theoretical estimates, discussed in the next section, can be made assuming a monodisperse distribution of final droplets with a radius of about 200 μm.

Discussion

The following discussion relates the experimental results to a simple theory assuming an instantaneous impulsive loading on the front face of the droplet. The mechanical impulse delivered to the droplet per unit frontal surface area $\mathcal{I}$ can be defined as follows:

$$(4/3)\pi R^3 \rho U = 2\pi R^2 \mathcal{I} \qquad (3)$$

where ρ is the drop density (1 g/cm^3) and U is the speed of the center of mass after impulse delivery and before air drag begins to slow the drop down. In writing Eq. (3) it is assumed that only a small fraction of the water is vaporized. U can be determined experimentally from $x-t$ diagrams of drop motion obtained from the fast framing movies. An example of such a diagram is shown in Fig. 8. Values of impulse inferred from these experiments using Eq. (3) show that $\mathcal{I} \geq 10$-20 dyn-s/cm^2 will produce shattering for drop radii between 0.01 and 0.15 cm.

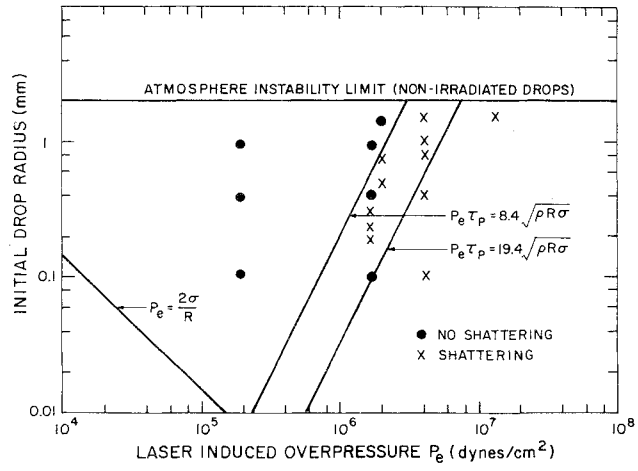

Fig. 5 Shattering limit vs calculated overpressure.

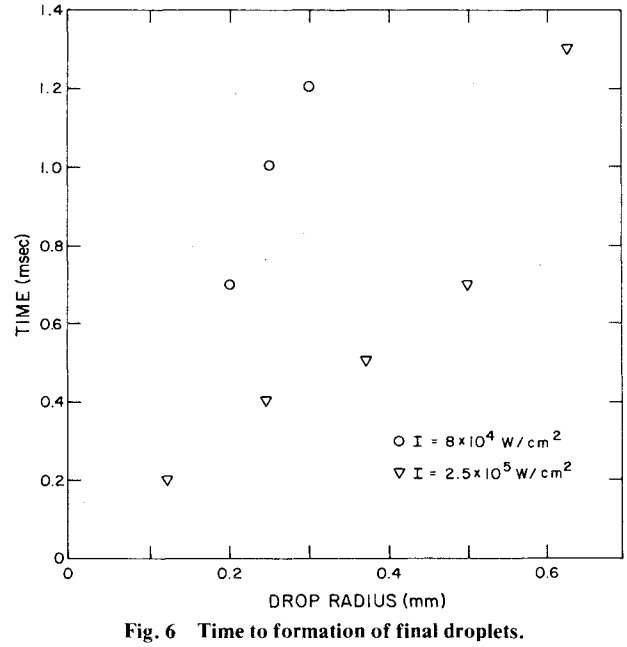

Fig. 6 Time to formation of final droplets.

The characteristic inertia, surface tension, and viscous forces acting on the fluid in a drop can now be estimated:

$$\text{inertia force} = \rho\left(\frac{\mathcal{I}}{\rho R}\right)^2 R^2 = \frac{\mathcal{I}^2}{\rho}$$

$$\text{surface tension force} = \sigma R$$

$$\text{viscous force} = \rho\nu\left(\frac{\mathcal{I}}{\rho R}/R\right)R^2 = \mathcal{I}\nu$$

where ν is the kinematic viscosity of water. The velocity relative to the center of mass is taken to be comparable to the velocity of the center of mass, so that it is of order $\mathcal{I}/\rho R$. The ratio of surface tension to inertia forces, $\rho R\sigma/\mathcal{I}^2$, is much greater than the ratio of viscous to inertia forces, $\rho\nu/\mathcal{I}$, for values of $\mathcal{I}$ of interest. Therefore, the dominant phenomenon involves a balance between inertia and surface tension.

Some interesting time estimates can be made. A characteristic droplet deformation time is $\rho R^2/\mathcal{I}$, the radius divided by the characteristic velocity derived above. If $\mathcal{I} = 10$-20 dyn-s/cm^2 the characteristic deformation time is 1-2 ms for $R = 0.15$ cm and 5-10 μs for $R = 0.01$ cm. Near the shattering

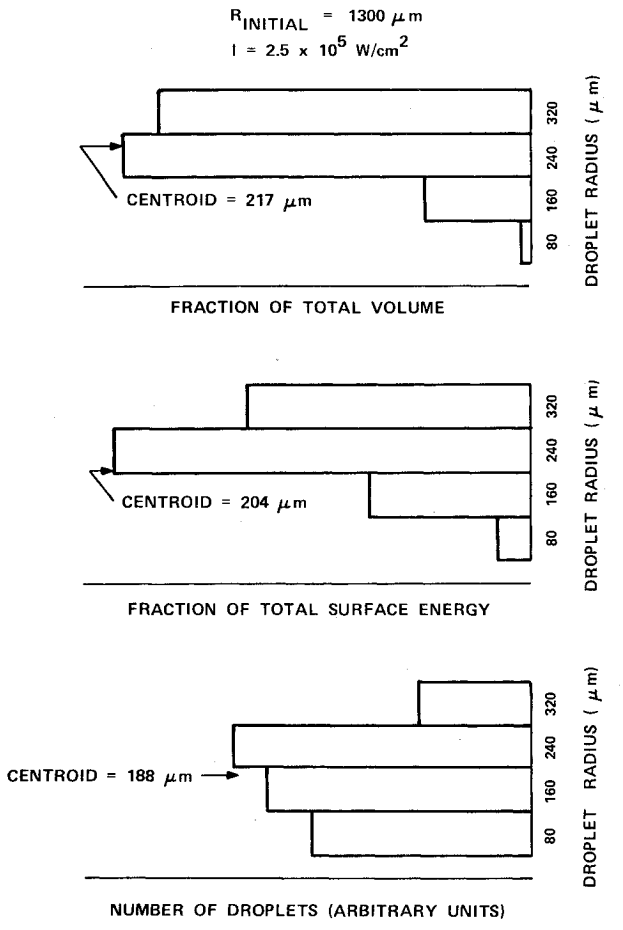

Fig. 7 Histograms for final droplets.

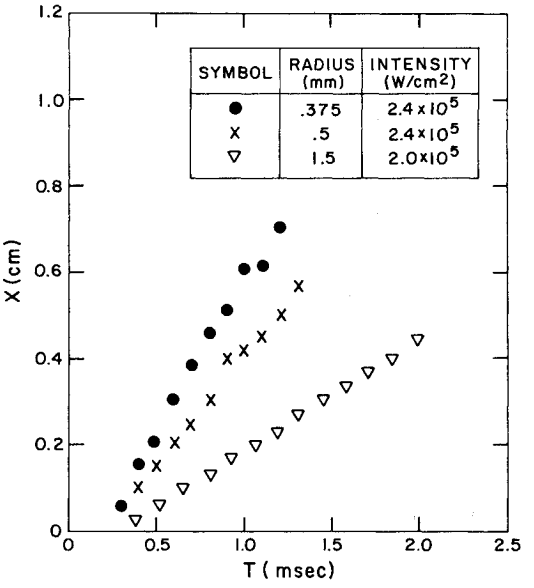

Fig. 8 Motion of droplet center of mass.

threshold it is reasonable to idealize the loading of a large droplet by the laser pulse as instantaneous. On the other hand, small droplets are in a transition regime for the 10 μs pulse duration used in these experiments. A theory has been developed only for the case of instantaneous impulsive loading on the droplet surface at time $t=0$.

In a center of mass frame of reference, the equations of motion for fluid within the drop are:

$$\text{div } v=0 \tag{4}$$

$$\rho\frac{dv}{dt}+\text{grad } p=0 \tag{5}$$

where v is the velocity vector. Mechanical energy balance for irrotational flow after an instantaneous pressure loading at $t=0$ is then

$$\frac{d}{dt}\int_V \frac{1}{2}\rho q^2 dv=-\oint_S pv_n dS \tag{6}$$

where $q^2=v\cdot v$, v_n is the normal velocity at the drop surface, and the integrals are over the drop volume and surface, respectively. Laplace's formula[5] gives

$$p=p_e+\sigma(K_1+K_2) \tag{7}$$

on the surface. Here K_1 and K_2 are the principal radii of curvature of the drop. No external work is done on the drop if the external pressure is uniform around the drop surface (after time $t=0_+$), and using Green's theorem Eq. (6) gives

$$\oint_S (\tfrac{1}{2}\rho\phi v_n+\sigma)dS=\text{const} \tag{8}$$

as the statement of mechanical energy conservation within the drop, where ϕ is the velocity potential ($v=\text{grad }\phi$). The constant in Eq. (8) can be evaluated by determining ϕ immediately after impulse delivery.

The velocity potential ϕ is found by assuming the impulse is delivered instantaneously to a spherical drop and that the instantaneous pressure loading on the surface has a cosine distribution:

$$p_e(\theta,t)=\begin{cases} 3\mathfrak{I}(\cos\theta)\delta(t), & 0\le\theta\le\pi/2 \\ 0, & \pi/2\le\theta\le\pi \end{cases} \tag{9}$$

where $\delta(t)$ is the Dirac delta function and θ is the angle between the radius vector at the drop surface and the laser direction. The cosine distribution is appropriate if the surface of the drop is a perfect absorber of the incident radiation. This is approximately correct. The loading is assumed to be axisymmetric. The number 3 in the pressure distribution is a consequence of integrating p_e to obtain the specific impulse $\mathfrak{I}$, defined in general by

$$\mathfrak{I}=\int_0^\pi\left[\int_{0_-}^{0_+} p_e(\theta,t)dt\right]\cos\theta\,\sin\theta d\theta \tag{10}$$

The pressure p_e can be expanded in the series

$$p_e=\delta(t)\sum_{n=0}^{\infty} A_nP_n\cos\theta \tag{11}$$

where the P_n are Legendre polynomials. The coefficients A_n are given by

$$A_n=3\mathfrak{I}(n+\tfrac{1}{2})\int_0^1 \zeta P_n(\zeta)d\zeta \tag{12}$$

The velocity potential satisfies $\nabla^2\phi=0$ and is related to the loading at the surface by the Bernoulli integral. Solution of this problem in spherical coordinates for instantaneous loading leads to the determination of ϕ and v_n on the drop surface. In a center of mass reference frame these are

$$\left.\begin{aligned}\phi&=-\frac{1}{\rho}\sum_{n=2}^{\infty}A_nP_n\cos\theta \\ v_n&=-\frac{1}{\rho R}\sum_{n=2}^{\infty}nA_nP_n\cos\theta\end{aligned}\right\}\text{ at } t=0_+ \tag{13}$$

The mechanical energy budget Eq. (8) reduces to

$$\oint (\tfrac{1}{2}\rho\phi V_n + \sigma)\,dS = \frac{\pi R}{\rho}\sum_{n=2}^{\infty}\frac{2n}{2n+1}A_n^2 + 4\pi R^2\sigma$$

$$= 4\pi R^2\sigma\left\{1 + \frac{9\mathcal{I}^2}{4\rho R\sigma}\sum_{n=2}^{\infty} n(n+\tfrac{1}{2})\left[\int_0^1 \zeta P_n(\zeta)\,d\zeta\right]\right\}^2 \qquad (14)$$

Note that the series in the last line of Eq. (14) is a pure number which can be evaluated numerically. The coefficient of $\mathcal{I}^2/\rho R\sigma$ is 0.205.

The final droplet size can now be calculated by postulating that in the final state there is no internal motion in the droplets, and therefore the initial internal kinetic energy in the original drop must be all converted to droplet surface energy. Assume that the final droplets are all of one radius R_f and that there are N droplets. Mass conservation requires $N=(R_0/R_f)^3$ if R_0 is the initial radius before the laser pulse caused shattering. This together with Eq. (14) leads to

$$R_f = R_0\Big/\left(1 + 0.205\,\frac{\mathcal{I}^2}{\rho R_0\sigma}\right) \qquad (15)$$

Equation (15) can be applied to the droplet shattering process considered in Figs. 4 and 7, in which case $R_0=0.13$ cm and $I=2.5\times10^5$ W/cm^2. We note that $\mathcal{I}=\bar{p}_e\tau_p$ and that $\bar{p}_e=p_{e_{max}}/3$ for a cosine distribution of overpressure, where the maximum value of overpressure occurs at $\theta=0$ and can be estimated using Eq. (2) and the laser intensity. Using this technique we find $\mathcal{I}=20$ dyn-s/cm^2 and $R_f=0.14$ mm. On the other hand, if the impulse is based on the center of mass velocity estimated from an $x-t$ diagram, we find $\mathcal{I}=16$ dyn-s/cm^2 and $R_f=0.21$ mm. The latter value of impulse should be more accurate. It is interesting to note that $\mathcal{I}$ scales with $I\tau_p$, and hence that the laser fluence, not the laser intensity, is the relevant parameter for short pulses. The final droplet radii estimated from Eq. (15) agree reasonably well with the centroids of the distributions in Fig. 7.

At this time we do not have a theoretical basis for establishing the critical impulse for shattering, but Eq. (15) provides a means of making an estimate. Suppose that only two drops of equal size result from the shattering process. In that case $(R_0/R_f)^3=2$ and $\mathcal{I}/\sqrt{\rho R\sigma}=1.13$ from Eq. (15). Thus, one would expect the shattering criterion to involve the parameter $\mathcal{I}/\sqrt{\rho R\sigma}$ exceeding a threshold value comparable to one. Lines of constant $p_e\tau_p/\sqrt{\rho R\sigma}$ are shown in Fig. 5 which define reasonable upper and lower bounds on the experimentally observed shattering threshold. The value of p_e should be understood to be the maximum overpressure because the surface was assumed normal to the beam in applying Eq. (2) to replot the results of Fig. 4 in Fig. 5. Thus, the shattering criterion based on experiment is $\mathcal{I}/\sqrt{\rho R\sigma}\geq 2.8$-6.5

It is not surprising that the experimental value would be higher than the estimate based on Eq. (15). There will actually be considerable internal motion in droplets after a laser pulse, and some of the mechanical energy can be dissipated over time scales long enough for viscous effects to be important. If enough energy has been dissipated and if the two droplets postulated above have remained close together, they can recoalesce into a droplet of the original size. We have observed this process in one film sequence for $I=8\times10^4$ W/cm^2.

The vapor blowoff will not be sonic, as assumed in deriving Eq. (2), at laser intensities less than about 10^5 W/cm^2. This tends to increase the slope of a line of constant $\mathcal{I}/\sqrt{\rho R\sigma}$ for smaller radii in Fig. 5. It is also true that small droplets ($R\sim0.1$ mm) are expected to deform significantly during the laser pulse, as discussed earlier. The shattering criterion is believed to be more nearly $\mathcal{I}/\sqrt{\rho R\sigma}\geq 3$ for an impulsive loading which can be considered instantaneous compared to a characteristic droplet deformation time.

Conclusions

For pulsed infrared laser propogation through rain, drops would be expected to shatter when the delivered specific impulse to the drop exceeds 10-20 dyn-s/cm^2 and pulse durations are short compared to pressure relaxation times between the front and rear surfaces. This corresponds roughly to a laser fluence of 1-2 J/cm^2. These criteria are expected to be independent of laser wavelength if the absorption length in liquid water is smaller than the drop diameter. Since rain drop radii are typically 0.1 cm, this phenomenon will not occur for wavelengths with absorption length of this order or larger.

A train of pulses would cause drops to cascade into smaller and smaller droplets until the radii are of the order of the absorption length (10 μm for 10.6 μm radiation). A laser with sufficient energy and flux to produce shattering would reduce rain to fog with a few pulses. The change in the size distribution function would lead to a greater surface to volume ratio for the liquid water in the beam path and hence reduce the time to completely vaporize the liquid water (i.e., burn through).

Acknowledgment

This work was supported under U.S. Navy Contract No. N00173-76-C-0059.

References

[1] Reilly, J., Singh, P., and Glickler, S., "Laser Interaction Phenomenology for Water Aerosols at CO_2 Laser Wavelengths," AIAA Paper 77-659, Albuquerque, N. Mex., June 1977.

[2] Knight, C., "Theoretical Modelling of Rapid Surface Vaporization with Back Pressure," *AIAA Journal*, Vol. 17, May 1979, pp. 519-523.

[3] Hanson, A., Domich, E., and Adams, H., "Shock Tube Investigation of the Breakup of Drops by Air Blasts," *The Physics of Fluids*, Aug. 1963, pp. 1070-1080.

[4] Lencioni, D., Henshaw, P., McSheehy, R., and DeGloria, D., "Pulsed Laser Propagation Through Aerosol Breakdowns," Project Report NLP-7, Lincoln Laboratory, Lexington, Mass., Dec. 17, 1976.

[5] Landau, L. and Lifshitz, E., *Fluid Mechanics*, Pergamon Press, New York, 1959, Chap. 7.